This is the author's version of an article that has been published in this journal. Changes were made to this version by the publisher prior to publication.
The final version of record is available at http://dx.doi.org/10.1109/TSP.2014.2307838

Fourier-Based Transmit Beampattern Design Using MIMO Radar

John Lipor, Sajid Ahmed, *Senior Member, IEEE*, and Mohamed-Slim Alouini, *Fellow, IEEE*

Abstract

In multiple-input multiple-output (MIMO) radar settings, it is often desirable to transmit power only to a given location or set of locations defined by a beampattern. Transmit waveform design is a topic that has received much attention recently, involving synthesis of both the signal covariance matrix, $\mathbf{R}$, as well as the actual waveforms. Current methods involve a two-step process of designing $\mathbf{R}$ via iterative solutions and then using $\mathbf{R}$ to generate waveforms that fulfill practical constraints such as having a constant-envelope or drawing from a finite alphabet. In this paper, a closed-form method to design $\mathbf{R}$ for a uniform linear array is proposed that utilizes the discrete Fourier transform (DFT) coefficients and Toeplitz matrices. The resulting covariance matrix fulfills the practical constraints such as positive semidefiniteness and the uniform elemental power constraint and provides performance similar to that of iterative methods, which require a much greater computation time. Next, a transmit architecture is presented that exploits the orthogonality of frequencies at discrete DFT values to transmit a sum of orthogonal signals from each antenna. The resulting waveforms provide a lower mean-square error than current methods at a much lower computational cost, and a simulated detection scenario demonstrates the performance advantages achieved.

Index Terms

This work was supported by a grant from the office of competitive research funding (OCRF) at King Abdullah University of Science and Technology (KAUST). This work will be presented in part at the IEEE International Conference on Acoustics, Speech and Signal Processing (ICASSP), Florence, Italy, May 2014.

J. Lipor was with the Computer, Electrical, Mathematical Sciences and Engineering (CEMSE) Division, KAUST, Thuwal, Makkah Province, Saudi Arabia. He is now with the Department of Electrical Engineering and Computer Science, University of Michigan, Ann Arbor, MI 48109 USA (e-mail: lipor@umich.edu).

S. Ahmed and M.-S. Alouini are with the Computer, Electrical, Mathematical Sciences and Engineering (CEMSE) Division, KAUST, Thuwal, Makkah Province, Saudi Arabia (e-mail: sajid.ahmed@kaust.edu.sa, slim.alouini@kaust.edu.sa).

Copyright (c) 2014 IEEE. Personal use is permitted. For any other purposes, permission must be obtained from the IEEE by emailing pubs-permissions@ieee.org.

This is the author's version of an article that has been published in this journal. Changes were made to this version by the publisher prior to publication.
The final version of record is available at http://dx.doi.org/10.1109/TSP.2014.2307838

Beampattern, discrete Fourier transform (DFT), multiple-input-multiple-output (MIMO) radar, waveform design.

I. Introduction

Multiple-input multiple-output (MIMO) radar has been a topic of interest for researchers in recent years due to the performance advantages offered over standard phased-array radar, including improved parameter identifiability and transmit beampattern matching [1]–[6]. For a MIMO system with widely-separated antennas [5], the spatial diversity of a target can be captured, resulting in improved signal-to-noise ratios (SNR) and high resolution target localization. In the case of co-located antennas [6], it has been shown that for a MIMO system with N_T transmit antennas, the number of targets that can be uniquely identified is N_T times the number of identifiable targets in a phased-array system. Moreover, the use of co-located antennas allows the user to design the signal covariance matrix such that the antennas transmit power only in a specified region [7]–[12]. In the traditional phased-array setup, each transmit antenna transmits a phase-shifted version of the same baseband waveform. In this case, the probing signals are fully correlated and the transmit covariance matrix is equal to unity everywhere, resulting in a single beam focused at the origin. A common MIMO setup is that of orthogonal or omnidirectional signaling, in which the antennas transmit mutually orthogonal waveforms. Here the transmit covariance matrix is equal to the identity matrix, and equal power is transmitted in all directions. The topic of transmit beampattern design lies between these two extremes and is the subject of this paper.

In the transmit beampattern design problem, the user wishes to transmit power exclusively to one or more prespecified regions of interest (ROIs). Previous work on beampattern design relies largely on iterative methods of solution [8]–[12]. In [9], the authors present a closed-form solution based on a least-squares cost function. However, the resulting covariance matrix is not positive semidefinite and therefore requires the use of eigenvalue or singular value decomposition. The solution also fails to fulfill the uniform elemental power constraint (i.e., it does not have constant values along the main diagonal). Another closed-form solution, which does fulfill these constraints, was presented in [7]. However, this method shows significant performance degradation compared with iterative methods, especially in the case of wide ROIs, and is only capable of transmitting power to a single ROI. One further method of closed-form beampattern design was presented as an initial guess in [11]. This method involves a summation of phased-array beams, but has the drawbacks of slow roll-off and high sidelobe levels. Efficient numerical solutions have been presented in [8], [10], [11], though for large array sizes these methods require a nontrivial amount of calculation time.

Copyright (c) 2014 IEEE. Personal use is permitted. For any other purposes, permission must be obtained from the IEEE by emailing pubs-permissions@ieee.org.

This is the author's version of an article that has been published in this journal. Changes were made to this version by the publisher prior to publication.
The final version of record is available at http://dx.doi.org/10.1109/TSP.2014.2307838

Once the covariance matrix has been designed, the next step is to design the actual waveforms to be transmitted that have the desired cross-correlations [13]–[15]. In [13], the authors extend the work of [8] to generate waveforms that fulfill realistic constraints such as the constant-envelope (CE) or low peak-to-average-power ratio (PAPR). However, the designed signals come from an infinite alphabet, and the method requires the use of an iterative solution. In [14], a mapping of Gaussian random variables into binary phase-shift keying (BPSK) and quadrature-phase shift keying (QPSK) CE waveforms is described. However, this method does not guarantee a positive semidefinite covariance matrix, and thus a second algorithm is proposed to generate BPSK waveforms that approximate a given covariance matrix. The work in [15] extends this method to QPSK signals. In both cases, iterative methods are again required, and the resulting beampatterns suffer from high sidelobe levels.

This paper involves two contributions. First, we present a novel closed-form method to synthesize the covariance matrix for the desired beampattern under the setting of a uniform linear array (ULA). The method relies on the simple procedure of choosing discrete Fourier transform (DFT) coefficients to have nonzero values, and then generating a Toeplitz matrix based on the corresponding discrete time signal. This method has the following advantages:

- The only operations involved are the computation of the DFT via the FFT algorithm and the generation of a Toeplitz matrix, both of which are computationally efficient.
- The practical constraints on $\mathbf{R}$ are shown to be fulfilled in the general case.
- The beampattern matching performance is similar to that achieved by iterative methods.

Second, we present a radar architecture that sums phase-shifted orthogonal signals in order to match the desired beampattern for the ULA. The proposed architecture provides a number of advantages over currently existing methods of waveform design, which are:

- The architecture does not require the generation of partially correlated waveforms or the use of iterative methods to do so, allowing for rapid generation of arbitrary beampatterns.
- The waveforms can be designed directly, allowing the user to omit the usual first step of designing the covariance matrix, $\mathbf{R}$.
- The achieved transmit beampattern matches exactly the theoretical beampattern calculated by the first algorithm.

This architecture has been demonstrated in the digital communications setting in [16], [17] and recently presented in the MIMO radar setting in [18]–[20]. In [18], the author uses a combination of phased-array beams as the basis to design the weight matrix and investigates the connections between this architecture

Copyright (c) 2014 IEEE. Personal use is permitted. For any other purposes, permission must be obtained from the IEEE by emailing pubs-permissions@ieee.org.

This is the author's version of an article that has been published in this journal. Changes were made to this version by the publisher prior to publication.
The final version of record is available at http://dx.doi.org/10.1109/TSP.2014.2307838

and classical (receive) array processing techniques. Our paper differs from this work in that we:

- Draw another important connection, namely between frequency sampling filter design and MIMO radar transmit beamforming, and then show how this relates to the standard phased-array beamformer.
- Consider the major practical concern of such a system, which is that of high PAPR, and provide a first analysis of the system.
- Demonstrate the benefits of the weighted orthogonal signaling over direct signal design through a detection scenario.

In [19], the design is focused on the application of subspace detection methods, such as multiple signal classification (MUSIC) and estimation of signal parameters via rotational invariance techniques (ESPRIT). Both closed-form and iterative solutions are presented. In this case, the closed-form solution fails to fulfill the uniform elemental power constraint, while the iterative solution has the obvious drawback of a higher required computational complexity. The work in [20] extends this paper to show how previously developed, iterative MIMO beamforming methods can be applied to the new architecture, but again invokes a costly computational burden. Neither paper includes an analysis of PAPR.

The remainder of this paper is organized as follows. Section II describes the MIMO radar signal model and the problem setup. Section III describes the proposed method for covariance matrix design and Section IV details the design of the actual transmit signals, which does not require the synthesis of the covariance matrix. Section V provides the theoretical computational complexity of the proposed algorithms. Simulation results are shown in Section VI, with conclusions given in Section VII.

II. Problem Formulation and Previous Work

Consider a MIMO radar system with N_T co-located transmit antennas in a ULA having interelement spacing d and transmission wavelength λ. Define the transmitted baseband signal vector as

$$\mathbf{x}(n) = \begin{bmatrix} x_1(n) & x_2(n) & \dots & x_{N_T}(n) \end{bmatrix}^T. \tag{1}$$

Assuming the transmitted probing signals are narrowband and that the propagation is nondispersive, the signal received by a target located at an angle θ at time n can be written as

$$r(n;\theta) = \mathbf{a}_T^H(\theta)\mathbf{x}(n), \tag{2}$$

where $(\cdot)^H$ denotes the conjugate transpose and $\mathbf{a}_T(\theta)$ represents the transmit steering vector, given by

$$\mathbf{a}_T(\theta) = \begin{bmatrix} 1 & e^{-j\frac{2\pi d}{\lambda}\sin(\theta)} & \dots & e^{-j\frac{2(N_T-1)\pi d}{\lambda}\sin(\theta)} \end{bmatrix}^T. \tag{3}$$

Copyright (c) 2014 IEEE. Personal use is permitted. For any other purposes, permission must be obtained from the IEEE by emailing pubs-permissions@ieee.org.

This is the author's version of an article that has been published in this journal. Changes were made to this version by the publisher prior to publication.
The final version of record is available at http://dx.doi.org/10.1109/TSP.2014.2307838

The transmitted power at location θ can then be found as

$$P(\theta) = \mathrm{E}\left\{\mathbf{a}_T^H(\theta)\mathbf{x}(n)\mathbf{x}^H(n)\mathbf{a}_T(\theta)\right\} = \mathbf{a}_T^H(\theta)\mathbf{R}\mathbf{a}_T(\theta), \tag{4}$$

where $\mathbf{R}$ is the covariance matrix of the transmitted waveforms and $\mathrm{E}\{\cdot\}$ denotes the expectation operator. The objective is to design $\mathbf{R}$ such that the transmitted power matches a desired beampattern as closely as possible while fulfilling the following constraints

$$C_1 : \mathbf{R} \geq 0$$

$$C_2 : \mathbf{R}(m,m) = c,\ m = 1, 2, ..., N_T,$$

where c is a constant equal to the power transmitted by each antenna. C_1 denotes the positive semidefinite constraint and C_2 denotes uniform elemental power constraint.

Previous work utilizes optimization techniques to minimize a variety of cost functions. The work in [8] formulates this problem as a semidefinite quadratic program (SQP) with a cost function involving a beampattern matching term and a cross-correlation term. In this paper, we ignore the cross-correlation term, in which case the objective function corresponds to the least-squares minimization problem defined as

$$J(\mathbf{R}) = \sum_{l=1}^{L}\left(\mathbf{a}_T^H(\theta_l)\mathbf{R}\mathbf{a}_T(\theta_l) - \alpha P_d(\theta_l)\right)^2, \tag{5}$$

where $P_d(\theta_l)$ is the desired beampattern defined over the grid points $\{\theta_l\}_{l=1}^{L}$, and α is a scaling factor. Minimization of this cost function can be achieved using freely available software [21], [22], where the constraints C_1 and C_2 can be trivially added.

In [11], the authors present unconstrained cost functions that can be solved using gradient-descent methods and do not necessarily rely on a quadratic cost function. In this case, C_1 is fulfilled by solving for the square-root matrix $\mathbf{U}$, such that $\mathbf{R} = \mathbf{U}^H\mathbf{U}$, and C_2 is fulfilled via a transformation to a hyperspherical coordinate system in order to force the norm of each column of $\mathbf{U}$ to be equal to c. The spherical transformation is represented by the parameterization of $\mathbf{U}$ by $\psi = \begin{bmatrix}\psi_{21} & \psi_{31} & \psi_{32} & \dots & \psi_{M,M-1}\end{bmatrix}^T$ (see [11] for further details). In this case, the cost function (5) is replaced by

$$J_1(\mathbf{\Theta}) = \sum_{l=1}^{L}\left(P(\psi,\theta_l) - \alpha P_d(\theta_l)\right)^2, \tag{6}$$

where $\Theta = \begin{bmatrix}\psi^T\alpha\end{bmatrix}^T$ and $P(\psi,\theta_l) = \mathbf{a}_T^H(\theta_l)\mathbf{U}^H(\psi)\mathbf{U}(\psi)\mathbf{a}_T(\theta_l)$. The authors also demonstrate the superior performance achieved by the 1-norm minimization by minimizing the cost function

$$J_2(\mathbf{\Theta}) = \sum_{l=1}^{L}\left|P(\psi,\theta_l) - \alpha P_d(\theta_l)\right|. \tag{7}$$

Copyright (c) 2014 IEEE. Personal use is permitted. For any other purposes, permission must be obtained from the IEEE by emailing pubs-permissions@ieee.org.

This is the author's version of an article that has been published in this journal. Changes were made to this version by the publisher prior to publication.
The final version of record is available at http://dx.doi.org/10.1109/TSP.2014.2307838

While many existing solutions rely on iterative methods to design the covariance matrix, closed-form solutions exist as well. In [7], rather than minimizing a cost function, the authors directly provide the cross-correlation between signals, which can be used to generate the covariance matrix. The cross-correlation is given as

$$r_{lm} = \frac{\sin\left[\pi\beta(l-m)\right]}{\sin\left[\pi\beta(l-m)/N_T\right]}. \tag{8}$$

In this case, the beamwidth of the resulting pattern is proportional to β, which can be varied from 0 to 1. The other closed-form method for generating covariance matrices appears in [11], but serves only as an approximation to the desired beampattern. The method utilizes a summation of phased-array beams at the angles within the desired ROIs, yielding the covariance matrix

$$\mathbf{R} = \frac{1}{L}\sum_{l=1}^{L} P_d(\theta_l)\mathbf{a}_T(\theta_l)\mathbf{a}_T^H(\theta_l). \tag{9}$$

While both of these methods provide closed-form solutions that fulfill both C_1 and C_2, neither results in performance that is comparable to that of the iterative methods. The motivation of the proposed work is therefore to provide a closed-form solution to the transmit beampattern matching problem that provides similar performance to iterative methods. We first propose a method of designing the covariance matrix through the use of DFT coefficients, and then show how the results can be used to design a system that can achieve arbitrary beampatterns through a combination of uncorrelated signals.

III. DFT-Based Covariance Matrix Design

In this section, we describe the proposed method of covariance matrix design, which exploits the DFT. By specifying a rectangular window (or set of windows) of varying width in the frequency domain, the user can equivalently achieve beampatterns of varying widths in the spatial domain. The method is similar to the familiar frequency sampling method for finite impulse response (FIR) filter design, which was noted as a method of receive (classical) beamforming in [23]. This further reinforces the similarities between filter design and MIMO radar transmit beamforming described in [7].

To establish the relationship between the rectangular window in the frequency domain and the desired beampattern, let $\{H(k)\}_{k=0}^{N_T-1}$ denote the frequency domain samples and $\{h(n)\}_{n=0}^{N_T-1}$ be the corresponding time domain samples obtained after applying the inverse DFT. The relationship between them can

Copyright (c) 2014 IEEE. Personal use is permitted. For any other purposes, permission must be obtained from the IEEE by emailing pubs-permissions@ieee.org.

This is the author's version of an article that has been published in this journal. Changes were made to this version by the publisher prior to publication.
The final version of record is available at http://dx.doi.org/10.1109/TSP.2014.2307838

be described by the N_T-point DFT operation as

$$H(k) = \sum_{n=0}^{N_T-1} h(n) e^{-j2\pi kn/N_T} \tag{10}$$

$$h(n) = \frac{1}{N_T} \sum_{k=0}^{N_T-1} H(k) e^{j2\pi kn/N_T}. \tag{11}$$

Using (10) and (11), the following lemma can be obtained.

Lemma 1: If $H(k)$ is an element of the set $\{0, 1\}$ for all k and $\mathbf{R}$ is the Toeplitz matrix formed using the samples $\{h(n)\}$ as

$$\mathbf{R} = \begin{bmatrix} h(0) & h(1) & \cdots & h(N_T-1) \\ h^*(1) & h(0) & \cdots & h(N_T-2) \\ h^*(2) & h^*(1) & \cdots & h(N_T-3) \\ \vdots & \vdots & \ddots & \vdots \\ h^*(N_T-1) & h^*(N_T-2) & \cdots & h(0) \end{bmatrix}, \tag{12}$$

then it can be easily proved that $\mathbf{R}$ will be positive semidefinite with maximum amplitude along the diagonal.

Proof: We begin by transforming $\mathbf{R}$ into a more convenient notation. Stack the elements $\{h(n)\}$ to obtain the column vector $\mathbf{h}$ with nth element

$$[\mathbf{h}]_n = \frac{1}{N_T} \sum_{k=0}^{N_T-1} H(k) e^{j2\pi kn/N_T}. \tag{13}$$

It can be noted here that for any window choice $[\mathbf{h}]_0 = \frac{1}{N_T} \sum_{k=0}^{N_T-1} H(k)$, which has maximum amplitude over all n. Let $\mathbf{h}_k$ be the contribution to the summation in (13) due to the kth value, i.e.,

$$[\mathbf{h}_k]_n = \frac{1}{N_T} H(k) e^{j2\pi kn/N_T}. \tag{14}$$

Then

$$\mathbf{h} = \sum_{k=0}^{N_T-1} \mathbf{h}_k, \tag{15}$$

and it is shown in Appendix A that

$$\mathbf{h}_k^H \mathbf{h}_l = \frac{1}{N_T} H(k)^2 \delta_{kl}, \tag{16}$$

where δ_{kl} is the Kronecker delta. Next, let $\{p_i\}_{i=1}^P$ be the set of values of k for which $H(k)$ is nonzero. In this case, $\mathbf{h}$ can be rewritten as

$$\mathbf{h} = \sum_{i=1}^{P} \mathbf{h}_{p_i}, \tag{17}$$

Copyright (c) 2014 IEEE. Personal use is permitted. For any other purposes, permission must be obtained from the IEEE by emailing pubs-permissions@ieee.org.

This is the author's version of an article that has been published in this journal. Changes were made to this version by the publisher prior to publication.
The final version of record is available at http://dx.doi.org/10.1109/TSP.2014.2307838

and it can be shown by inspection that the resulting Toeplitz matrix created using $\mathbf{h}$ is equivalent to

$$\mathbf{R} = N_T \sum_{i=1}^{P} \mathbf{h}_{p_i}^* \mathbf{h}_{p_i}^T. \tag{18}$$

For any arbitrary vector $\mathbf{g}$ of corresponding length, we can write

$$\begin{aligned} \mathbf{g}^H \mathbf{R} \mathbf{g} &= N_T \sum_{i=1}^{P} \mathbf{g}^H \mathbf{h}_{p_i}^* \mathbf{h}_{p_i}^T \mathbf{g} \\ &= \sum_{i=1}^{P} |\mathbf{g}^H \mathbf{h}_{p_i}|^2 \end{aligned}$$

which is real and nonnegative for all $\mathbf{g}$. Thus the proposed matrix is positive semidefinite for all $H(k) \in \{0, 1\}$. Also note that since $\mathbf{R}$ is a summation of P rank-1 matrices, its rank will be at most P. ■

Lemma 2: If $H(k)$ is real and $\mathbf{R}$ is the Toeplitz matrix formed using the samples $\{h(n)\}$ as in *Lemma 1*, then it can be easily proved that

$$\mathbf{e}^H(k) \mathbf{R} \mathbf{e}(k) = N_T H(k), \tag{19}$$

where

$$\mathbf{e}(k) = \begin{bmatrix} 1 & e^{-j\frac{2\pi k}{N_T}} & \dots & e^{-j\frac{2\pi k(N_T-1)}{N_T}} \end{bmatrix}^T \tag{20}$$

is the Fourier vector corresponding to frequency k.

Please see Appendix B for proof.

Using *Lemma 2*, we can write

$$\sum_{k=0}^{N_T-1} \left(\mathbf{e}^H(k) \tilde{\mathbf{R}} \mathbf{e}(k) - \frac{N_T}{h(0)} H(k) \right)^2 = 0, \tag{21}$$

where the matrix $\tilde{\mathbf{R}} = \frac{\mathbf{R}}{h(0)}$ is the normalized covariance matrix. Since $\mathbf{e}(k)$ is similar to the steering vector $\mathbf{a}_T(\theta_k)$ and $\tilde{\mathbf{R}}$ is a covariance matrix, the expression (21) is similar to the cost function (5) of the beampattern design problem to synthesize the covariance matrix. Therefore, considering $H(k)$ as the desired transmit beampattern and $\mathbf{e}^H(k) \tilde{\mathbf{R}} \mathbf{e}(k)$ as the designed beampattern at discrete point k, the transmit beampattern design problem can be mapped onto (21) to find the waveform covariance matrix.

In order to map the discrete frequency point, k, onto the positive and negative spatial locations of θ_k, note that k denotes both positive and negative frequency points. The following relationship can be used to map the frequency components onto the spatial domain for an even number of transmit antennas

$$\theta_k = \begin{cases} \sin^{-1}\left(\frac{\lambda k}{d N_T}\right), & k = 0, \dots, \frac{N_T}{2} \\ -\sin^{-1}\left(\frac{\lambda (N_T - k)}{d N_T}\right), & k = \frac{N_T}{2} + 1, \dots, N_T - 1 \end{cases}. \tag{22}$$

Copyright (c) 2014 IEEE. Personal use is permitted. For any other purposes, permission must be obtained from the IEEE by emailing pubs-permissions@ieee.org.

This is the author's version of an article that has been published in this journal. Changes were made to this version by the publisher prior to publication.
The final version of record is available at http://dx.doi.org/10.1109/TSP.2014.2307838

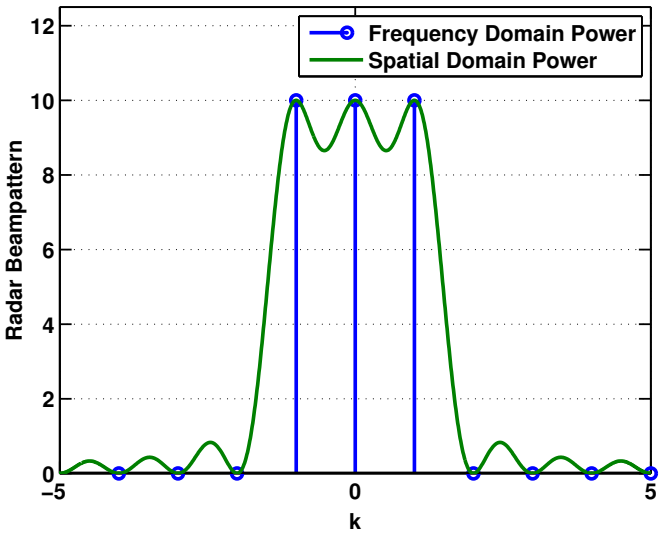

Fig. 1. Resulting beampattern in frequency and spatial domains using the proposed DFT design method with $N_T = 10$ and $H(k) = 1,\ k = 0, 1, 9$.

Simlarly, the mapping for an odd number of transmit antennas is

$$\theta_k = \begin{cases} \sin^{-1}\left(\frac{\lambda k}{dN_T}\right), & k = 0, \ldots, \lfloor \frac{N_T}{2} \rfloor \\ -\sin^{-1}\left(\frac{\lambda (N_T - k)}{dN_T}\right), & k = \lceil \frac{N_T}{2} \rceil + 1, \ldots, N_T - 1 \end{cases}, \tag{23}$$

where $\lfloor \cdot \rfloor$ and $\lceil \cdot \rceil$ denote the floor and ceiling, respectively.

Given the above mappings, it can be seen that a window in the frequency (k) domain results in a window of proportional width in the spatial (θ) domain. In the two extremes of a single nonzero point at $k = 0$ and a vector of all non-zero points, the beampattern results in the phased-array and omnidirectional patterns, respectively. Fig. 1 shows the frequency domain and spatial domain power in the case of $N_T = 10$ with half-wavelength interelement spacing and a window with $H(k) = 1,\ k = 0, 1, 9$. The resulting beampattern has amplitude 10 at 0° and $\pm 11.54^\circ$.

While the beampattern matches (19) for spatial values corresponding to integer values of k, the function does not describe the beampattern for other values of θ. We now demonstrate that choosing the positive coefficients in the window function is equivalent to adding phased-array beams with centers at the given locations. We begin by noting that a covariance matrix to generate P phased-array beams with centers

Copyright (c) 2014 IEEE. Personal use is permitted. For any other purposes, permission must be obtained from the IEEE by emailing pubs-permissions@ieee.org.

This is the author's version of an article that has been published in this journal. Changes were made to this version by the publisher prior to publication.
The final version of record is available at http://dx.doi.org/10.1109/TSP.2014.2307838

located at $\{\theta_i\}_{i=1}^P$, can be equivalently designed by creating a Toeplitz matrix as in (12) using the vector

$$\begin{aligned}\tilde{\mathbf{a}} &= \sum_{i=1}^{P} \mathbf{a}_T^*(\theta_i) \\ &= \sum_{i=1}^{P} \left[1 \quad e^{j\frac{2\pi d}{\lambda}\sin(\theta_i)} \quad \ldots \quad e^{j\frac{2(N_T-1)\pi d}{\lambda}\sin(\theta_i)}\right]^T, \end{aligned} \tag{24}$$

to define the first row, or through a summation of phased-array covariance matrices

$$\mathbf{R} = \sum_{i=1}^{P} \mathbf{a}_T(\theta_i)\mathbf{a}_T^H(\theta_i). \tag{25}$$

It has been shown [24] that for receive beamformers, many widely used methods are composed of a summation of conventional (uniformly weighted) beamformers with centers at various locations. On the transmit side, the conventional beamformer corresponds to the phased-array beam (see Appendix C). The method presented in [11] (defined by (9)) shows that the sum of phased-array beams provides a suitable guess at the covariance matrix needed to match a given beampattern. However, in this case the sidelobes levels are high and the main lobe suffers from slow roll-off due to the high number of beams in the summation. Thus, performance benefits can be achieved by choosing a lower number of beams to sum. For the frequency-domain window with P unity coefficients at locations $\{p_i\}_{i=1}^P$, the transformed coefficients are

$$\begin{aligned} h(n) &= \frac{1}{N_T}\sum_{i=1}^{P} e^{j2\pi p_i n/N_T} \\ &= \frac{1}{N_T}\sum_{i=1}^{P} e^{j\frac{2\pi dn}{\lambda}\sin(\theta_i)}, \end{aligned} \tag{26}$$

where $\{\theta_i\}_{i=1}^P$ is the set of locations corresponding to $\{p_i\}_{i=1}^P$ and is found by solving (22). Vectorizing over all values of n, we obtain the frequency and spatial domain vectors

$$\mathbf{h} = \frac{1}{N_T}\sum_{i=1}^{P} \left[1 \quad e^{j2\pi p_i/N_T} \quad \ldots \quad e^{j2\pi p_i(N_T-1)/N_T}\right]^T \tag{27}$$

$$= \frac{1}{N_T}\sum_{i=1}^{P} \left[1 \quad e^{j\frac{2\pi d}{\lambda}\sin(\theta_i)} \quad \ldots \quad e^{j\frac{2\pi d(N_T-1)}{\lambda}\sin(\theta_i)}\right]^T. \tag{28}$$

It is easily seen that $\mathbf{h}$ as described in (28) corresponds to a scaled version of (24). For this reason, we conclude that the method of choosing beam locations using P DFT coefficients is equivalent to a sum of P phased array beams. Since the DFT coefficients represent mutually orthogonal frequencies, the resulting beams are placed at the nulls of the other beams in the sum, resulting in a smooth function

Copyright (c) 2014 IEEE. Personal use is permitted. For any other purposes, permission must be obtained from the IEEE by emailing pubs-permissions@ieee.org.

This is the author's version of an article that has been published in this journal. Changes were made to this version by the publisher prior to publication.
The final version of record is available at http://dx.doi.org/10.1109/TSP.2014.2307838

Algorithm 1 Method of choosing $\{p_i\}_{i=1}^{P}$ for a given ROI

input: $P_d(\theta)$

$\theta_{max} = \max\{\theta \in \text{ROI}\}$

$\theta_{min} = \min\{\theta \in \text{ROI}\}$

solve (22) or (23) to obtain $k_{\max}$ corresponding to θ_{max} and $k_{\min}$ corresponding to θ_{min}

$k^+ \leftarrow \lfloor k_{\max} \rfloor$

$k^- \leftarrow \lceil k_{\min} \rceil$

$\{p_i\} = \{k \in \mathbb{Z} \mid k^- \leq k \leq k^+\}$

within the window and overlapping sidelobes and nulls outside the ROI. In order to choose the values of k that define $\{p_i\}_{i=1}^{P}$ for a given ROI, Algorithm 1 can be employed.

The main drawback of the method as proposed is that there are only N_T degrees of freedom available for beampattern design. Therefore, arrays with a low number of transmit antennas will only be able to transmit beams with a limited number of widths. However, with recent advances in sensor technology, the number of transmit antennas in systems has grown significantly. In such systems, the achievable resolution will be sufficient. The available resolution can be characterized by the null-to-null beamwidth, BW_{NN}. For a single phased-array beam, it is proved in Appendix C that

$$BW_{NN-PA} = 2\sin^{-1}\left(\frac{2\lambda}{dN_T}\right). \tag{29}$$

This describes the minimum beamwidth achievable for any radar setup. Let θ_{k^+} be the greatest value of θ in the ROI, corresponding to $k = k^+$ as defined by (22) or (23). Similarly, let θ_{k^-} be the smallest value of θ in the ROI, corresponding to $k = k^-$. Since the proposed method involves a summation of phased-array beams, the overall beamwidth is easily found to be

$$BW_{NN} = \theta_{k=k^++1} + \theta_{k=k^--1}. \tag{30}$$

For example, for the beampattern pictured in Fig. 1, $k^+ = 1$ and $k^- = 9$, and therefore

$$\begin{aligned} BW_{NN} &= \theta_{k=2} + \theta_{k=8} \\ &\approx 47.16^\circ. \end{aligned} \tag{31}$$

The other problem with the proposed method is that the resulting covariance matrix is rank-deficient and equal to the number of nonzero values of $H(k)$ (see proof of *Lemma 1*), reducing the total number of resolvable targets. However, since beamforming is often performed to account for some ambiguity in

Copyright (c) 2014 IEEE. Personal use is permitted. For any other purposes, permission must be obtained from the IEEE by emailing pubs-permissions@ieee.org.

This is the author's version of an article that has been published in this journal. Changes were made to this version by the publisher prior to publication.
The final version of record is available at http://dx.doi.org/10.1109/TSP.2014.2307838

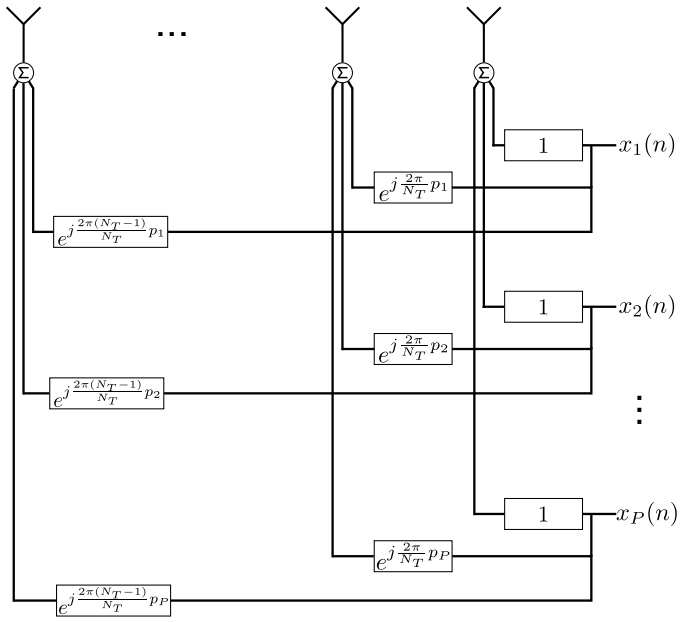

Fig. 2. Architecture of proposed system capable of matching a desired beampattern using orthogonal waveforms.

the location of a single target or limited number of targets [12], we conclude that the rank deficiency is a worthwhile tradeoff given the computational gains achieved by the proposed method.

IV. Transmit Signal Design

In this section, a method of directly designing transmit waveforms to achieve the beampattern which is obtained by synthesizing $\mathbf{R}$ in the previous section is described. While it is possible to stop with the covariance matrix designed in Section III and use the techniques presented in [13]–[15] to select waveforms, the architecture presented here does not rely on iterative methods of solution and can thus be employed for rapid transmission of arbitrary beampatterns.

Consider an arbitrary $H(k)$ used to define a desired transmit window and its corresponding vector $\mathbf{h}$ as described by (27). As demonstrated in (18) and (16), the transmit covariance matrix can be written as a sum of P rank-1 matrices defined by mutually orthogonal column vectors. Because of this fact, the beampattern can be achieved by transmitting a combination of P orthogonal sets of symbols drawn from any modulation scheme (e.g., BPSK or QPSK). Let $x_i(n)$ represent the symbol at time n that is weighted by the vector $\mathbf{h}_{p_i}$, and let $h_{p_i}(m)$ denote the mth element of $\mathbf{h}_{p_i}$. The proposed architecture,

Copyright (c) 2014 IEEE. Personal use is permitted. For any other purposes, permission must be obtained from the IEEE by emailing pubs-permissions@ieee.org.

This is the author's version of an article that has been published in this journal. Changes were made to this version by the publisher prior to publication.
The final version of record is available at http://dx.doi.org/10.1109/TSP.2014.2307838

as shown in Fig. 2, transmits the following signal from antenna m at time n

$$v_m(n) = \sum_{i=1}^{P} x_i(n) h_{p_i}(m). \tag{32}$$

The average power transmitted from antenna m is then found to be

$$\begin{aligned} P_{avg}(m) &= \mathrm{E}\left\{v_m(n) v_m^*(n)\right\} && (33)\\ &= \mathrm{E}\left\{\left|\sum_{i=1}^{P} x_i(n) h_{p_i}(m)\right|^2\right\} \\ &= \mathrm{E}\left\{\sum_{i=1}^{P}\sum_{l=1}^{P} x_i(n) x_l^*(n) h_{p_i}(m) h_{p_l}^*(m)\right\} \\ &= \sum_{i=1}^{P}\sum_{l=1}^{P} \mathrm{E}\left\{x_i(n) x_l^*(n)\right\} h_{p_i}(m) h_{p_l}^*(m) \\ &= \sum_{i=1}^{P} h_{p_i}(m) h_{p_i}^*(m) \\ &= \frac{P}{N_T^2}, && (34) \end{aligned}$$

where we have made use of (16) to eliminate the double summation, set $H(k) = 1$ for $k \in \{p_i\}_{i=1}^{P}$, and assumed the transmitted symbols to be orthonormal. From (34), one can see that the transmitted power is independent of the antenna number, demonstrating that the uniform elemental power constraint is fulfilled. The instantaneous power transmitted by antenna m at time n is

$$P_{inst}(m;n) = v_m(n) v_m^*(n) = \sum_{i=1}^{P}\sum_{l=1}^{P} x_i(n) x_l^*(n) h_{p_i}(m) h_{p_l}^*(m). \tag{35}$$

Another important practical consideration is that of PAPR, which is defined for antenna m by

$$\mathrm{PAPR}(m) = \frac{\max_n P_{inst}(m;n)}{P_{avg}(m)}. \tag{36}$$

When transmitting BPSK symbols, the peak instantaneous power occurs when all symbols are equal to one, resulting in

$$\begin{aligned} P_{peak}(m) &= \sum_{i=1}^{P}\sum_{l=1}^{P} h_{p_i}(m) h_{p_l}^*(m) \\ &= \frac{1}{N_T^2}\sum_{i=1}^{P}\sum_{l=1}^{P} e^{j\frac{2\pi m(p_i - p_l)}{N_T}}. && (37) \end{aligned}$$

From (37), it can be seen that the maximum instantaneous power occurs when $m = N_T$, in which case the instantaneous power is P^2/N_T^2 and the resulting PAPR is P. However, for $m \neq N_T$, the PAPR is less than P.

Copyright (c) 2014 IEEE. Personal use is permitted. For any other purposes, permission must be obtained from the IEEE by emailing pubs-permissions@ieee.org.

This is the author's version of an article that has been published in this journal. Changes were made to this version by the publisher prior to publication.
The final version of record is available at http://dx.doi.org/10.1109/TSP.2014.2307838

Using this setup, the signal received by a target located at angle θ at time n becomes

$$r(n;\theta) = \sum_{i=1}^{P} \mathbf{h}_{p_i}^T \mathbf{a}_T(\theta) x_i(n). \tag{38}$$

Let S be the total number of symbols transmitted and $\mathbf{x}_i$ be the column vector of S symbols. Define the symbol and weight matrices as

$$\mathbf{X} = \begin{bmatrix} \mathbf{x}_1 & \mathbf{x}_2 & \dots & \mathbf{x}_P \end{bmatrix}_{P\times S}^T \tag{39}$$

and

$$\mathbf{H} = \begin{bmatrix} \mathbf{h}_{p_1} & \mathbf{h}_{p_2} & \dots & \mathbf{h}_{p_P} \end{bmatrix}_{P\times N_T}^T, \tag{40}$$

respectively. Vectorizing the received symbols, the received signal from angle θ can be written as

$$\begin{aligned} \mathbf{r}(\theta) &= \begin{bmatrix} r(0;\theta) & r(1;\theta) & \cdots & r(S-1;\theta) \end{bmatrix}^T \\ &= \mathbf{X}^T \mathbf{H} \mathbf{a}_T(\theta). \end{aligned} \tag{41}$$

The power delivered to angle θ is then

$$\begin{aligned} P(\theta) &= \mathrm{E}\left\{ \mathbf{a}_T^H(\theta) \mathbf{H}^H \mathbf{X}^* \mathbf{X}^T \mathbf{H} \mathbf{a}_T(\theta) \right\} \\ &= \mathbf{a}_T^H(\theta) \mathbf{H}^H \mathbf{H} \mathbf{a}_T(\theta). \end{aligned} \tag{42}$$

The resulting system is a cross between phased-array and MIMO systems in which the number of uncorrelated waveforms is $P \leq N_T$. The proposed system provides benefits over the waveform design methods presented in [13]–[15] in that it does not require the generation of partially correlated symbols and therefore has a much lower computational cost. Rather, the transmitted signals can be designed directly, and the initial step of designing the covariance matrix can be omitted. In addition, transmission of truly orthogonal signals (e.g., BPSK symbols drawn from Hadamard code sequences) allows the transmitted beampattern to match the theoretical beampattern achieved by the covariance design procedure in the previous section.

V. Computational Complexity

A. Covariance Matrix Design

The only operations required for the proposed covariance matrix design are the FFT and the generation of a Toeplitz matrix. The complexity of the N-point FFT is well known and equal to $O\left(N\log(N)\right)$ computations. The complexity of generating a Toeplitz matrix is considered negligible, yielding an overall complexity of $O\left(N_T\log(N_T)\right)$. As a comparison, the SQP algorithm from [8] has a complexity of $O\left(\log\left(\frac{1}{\eta}\right) N_T^{3.5}\right)$ for a prefixed accuracy of η [14].

Copyright (c) 2014 IEEE. Personal use is permitted. For any other purposes, permission must be obtained from the IEEE by emailing pubs-permissions@ieee.org.

This is the author's version of an article that has been published in this journal. Changes were made to this version by the publisher prior to publication.
The final version of record is available at http://dx.doi.org/10.1109/TSP.2014.2307838

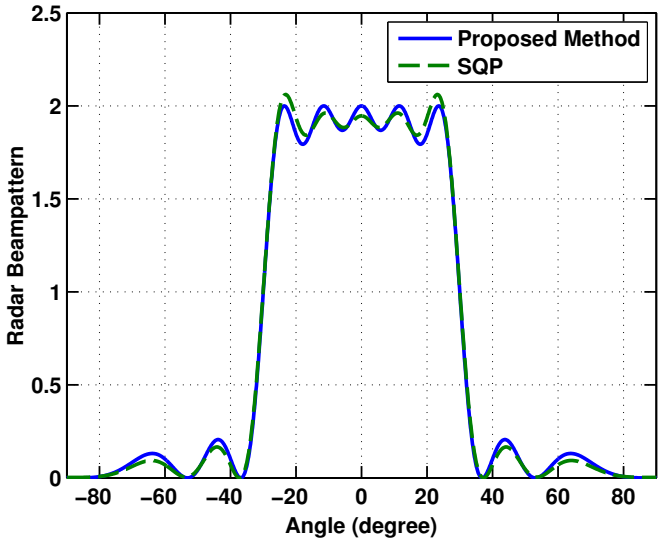

Fig. 3. Comparison of beampatterns achieved by proposed method of covariance matrix design with $H(k) = 1,\ k = 0, 1, 2, 8, 9$ and SQP method. The ROI is $\theta \in [-30^\circ, 30^\circ]$ and $N_T = 10$.

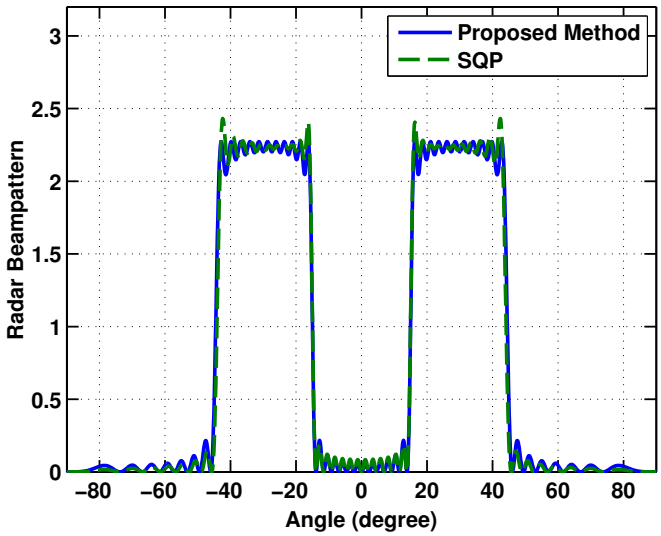

Fig. 4. Beampattern achieved through covariance matrix design for $N_T = 50$ with $H(k) = 1,\ k = 8 - 18, 34 - 44$. The corresponding ROIs are $\theta \in [-44, -15] \cup [15, 44]$.

B. Transmit Signal Design

Once the orthogonal symbols are obtained, the proposed radar architecture requires P complex multiplications and P complex additions per symbol for each antenna. Therefore, the total number of

Copyright (c) 2014 IEEE. Personal use is permitted. For any other purposes, permission must be obtained from the IEEE by emailing pubs-permissions@ieee.org.

This is the author's version of an article that has been published in this journal. Changes were made to this version by the publisher prior to publication.
The final version of record is available at http://dx.doi.org/10.1109/TSP.2014.2307838

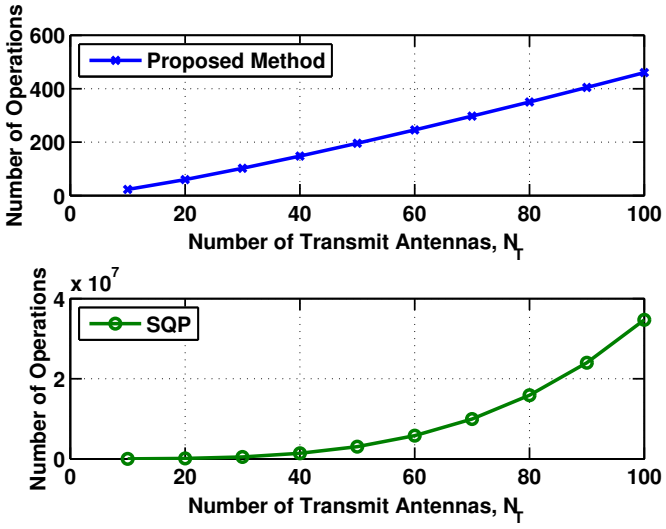

Fig. 5. Complexity required to generate $\mathbf{R}$ as a function of the number of transmit antennas.

operations required for S symbols transmitted from N_T antennas is SPN_T real multiplications and SPN_T real additions. Since this method does not require $\mathbf{R}$ to be generated before the transmit signals are designed, this represents the total computational complexity of the architecture. In comparison, the algorithm proposed in [13] requires $O\left(S + 3SN_T^2\right)$ operations per iteration after generating $\mathbf{R}$ (incurring the computational cost described above). The efficient algorithm presented in [14] requires an overall complexity of $\sum_{m=3}^{N_T} m + \frac{N_T(N_T^2-N_T)}{2} + L\left(\frac{(N_T-1)(N_T^2-N_T)}{2} + (2N_T^2+4N_T)\right)$ operations per iteration and $O\left(N_T^3 + SN_T^2\right)$ real multiplications to find both the covariance matrix and the BPSK symbols.

VI. Simulation Results

In this section we present numerical examples to demonstrate the performance of the design methods described. Simulations assume a uniform linear array with half-wavelength interelement spacing and a mesh grid with spacing of 0.1°.

We begin by demonstrating the performance of the method for covariance matrix design presented in Section III. Fig. 3 shows the resulting beampattern with $N_T = 10$ transmit antennas for the ROI defined by $\theta \in [-30^\circ, 30^\circ]$. Employing Algorithm 1, we obtain $\{p_i\} = \{0, 1, 2, 8, 9\}$ and set $H(k) = 1$ for these values of k. The solution found using the SQP as presented in [8] is also included for comparison. The total transmit power is normalized to unity. The theoretical BW_{NN} for the proposed method is

$$BW_{NN} = \theta_{k=3} + \theta_{k=7} \approx 73.7^\circ, \tag{43}$$

Copyright (c) 2014 IEEE. Personal use is permitted. For any other purposes, permission must be obtained from the IEEE by emailing pubs-permissions@ieee.org.

This is the author's version of an article that has been published in this journal. Changes were made to this version by the publisher prior to publication.
The final version of record is available at http://dx.doi.org/10.1109/TSP.2014.2307838

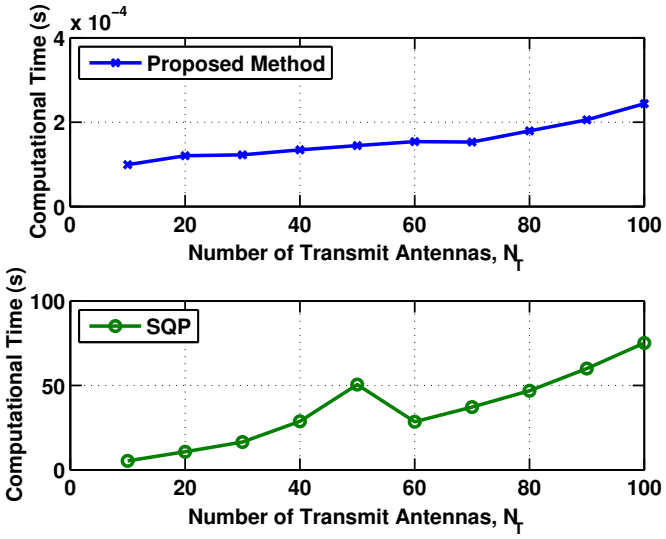

Fig. 6. Computational time required to generate $\mathbf{R}$ as a function of the number of transmit antennas.

which matches the simulated value exactly. For the SQP method, the resulting $BW_{NN} \approx 74.6°$. It can be seen that the proposed method provides similar performance to the iterative solution. Define the mean-squared error (MSE) as

$$\text{MSE} = \frac{1}{L}\sum_{l=1}^{L}\left[P(\theta_l) - \alpha\phi(\theta_l)\right]^2, \tag{44}$$

where α is found using the SQP method. The resulting mean-squared errors (MSEs) are 0.0322 for the proposed method and 0.0311 for the SQP method. Thus, we conclude that the proposed method provides performance which is comparable to that achieved by iterative methods while incurring a fraction of the computational cost. Fig. 4 shows the resulting beampattern for $N_T = 50$ with ROIs defined by $\theta \in [-44°, -15°] \cup [15°, 44°]$. Employing Algorithm 1 results in $H(k) = 1,\ k = 8-18,\ 34-44$. The resulting MSEs are 0.0230 and 0.0175 for the proposed and SQP methods, respectively. Fig. 5 shows the computational complexity (as defined in Section V) as a function of the number of transmit antennas for both the proposed and SQP methods with $\eta = 0.0311$. The results are shown in subfigures due to the difference in scale, and the figures demonstrate the clear computational advantage of the proposed method, especially as the number of transmit antennas becomes large. To further demonstrate the difference in required computational time, we show a comparison of average run time required to generate the beampattern pictured in Fig. 3. Fig. 6 shows the average run time required over 500 Monte Carlo simulations on a personal computer running MATLAB. The figure reinforces the computational advantage of the proposed method.

Copyright (c) 2014 IEEE. Personal use is permitted. For any other purposes, permission must be obtained from the IEEE by emailing pubs-permissions@ieee.org.

This is the author's version of an article that has been published in this journal. Changes were made to this version by the publisher prior to publication.
The final version of record is available at http://dx.doi.org/10.1109/TSP.2014.2307838

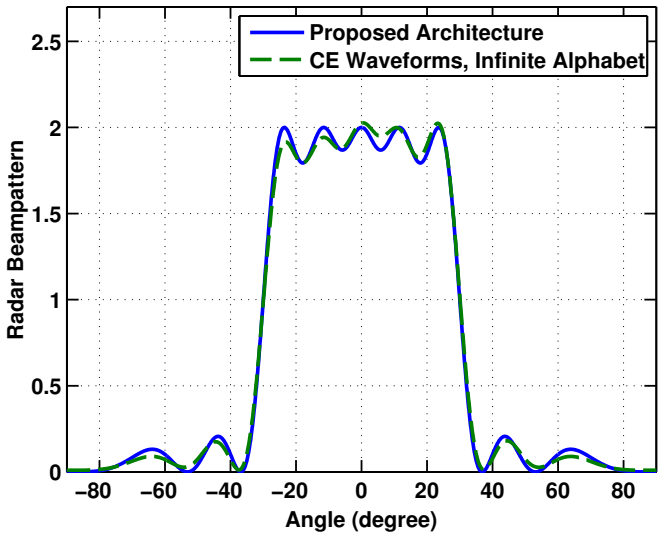

Fig. 7. Beampatterns achieved by transmitting symbols via the proposed architecture and the CE waveforms obtained using the cyclic algorithm from [13].

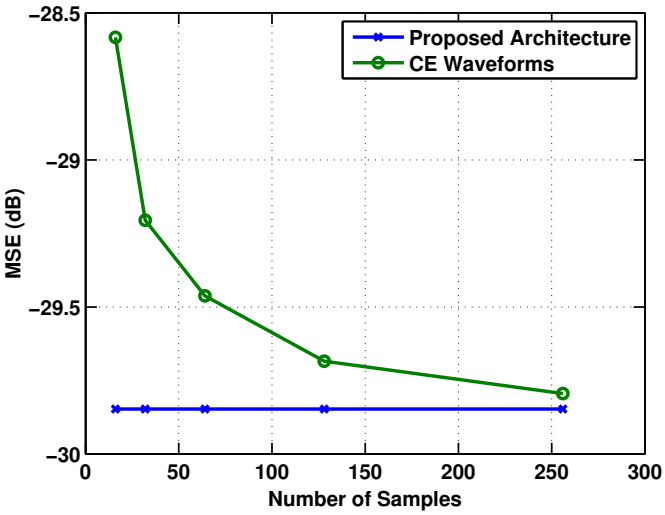

Fig. 8. MSE of transmitted power as a function of the number of samples when transmitting symbols via the proposed architecture and the cyclic algorithm from [13] with PAPR = 1.

Next, we demonstrate the performance achieved by the proposed radar architecture in Section IV. Fig. 7 shows the beampattern generated using the proposed method with orthogonal BPSK symbols drawn from Hadamard code sequences of length 128. The resulting beampattern formed using the CE waveforms described in [13] with PAPR = 1 is included for comparison (note that these waveforms come from an

Copyright (c) 2014 IEEE. Personal use is permitted. For any other purposes, permission must be obtained from the IEEE by emailing pubs-permissions@ieee.org.

This is the author's version of an article that has been published in this journal. Changes were made to this version by the publisher prior to publication.
The final version of record is available at http://dx.doi.org/10.1109/TSP.2014.2307838

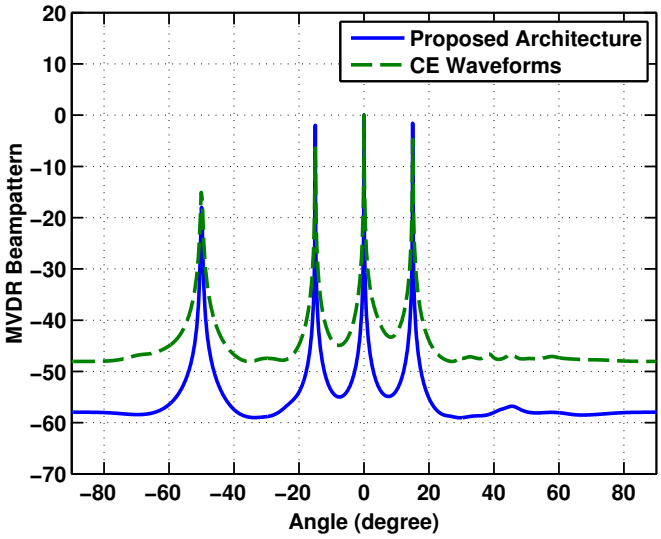

Fig. 9. Receive beampatterns after applying the MVDR beamformer for multiple targets of interest using the proposed architecture and the CE waveforms generated by [13].

infinite alphabet). The desired beampattern is the same as in Fig. 3, and the resulting MSEs obtained by averaging over 100 Monte Carlo trials are 0.0322 for the proposed method and 0.0328 for the SQP. Thus, the proposed method provides a lower MSE and utilizes symbols from a finite alphabet while incurring a much lower computational cost. Fig. 8 shows the MSE as a function of the number of samples when transmitting via the proposed method and the method presented in [13]. Since it is possible to generate truly orthogonal BPSK symbols, the proposed method results in a uniform MSE regardless of the number of samples. The proposed method also requires a negligible computational time compared to the iterative methods used in [13]–[15]. Moreover, the proposed architecture does not require the user to generate the theoretical covariance matrix prior to designing the actual waveforms, which can present a large computational cost as demonstrated in Fig. 5.

We conclude this section by demonstrating the receive beampattern after applying the adaptive minimum variance distortionless response (MVDR) or Capon beamformer. Consider the scenario in which there are three targets of interest located at 0° and $\pm 15^\circ$ and one interfering target located at -50° that we desire to suppress. Probing signals are transmitted using the proposed radar architecture and the method presented in [13] with the same desired beampattern as in Figs. 3 and 7. The total transmit power is equal to 1. The received signal is corrupted by white Gaussian noise with a variance equal to 0.01. Fig. 9 shows the average resulting beampatterns from the two methods after transmitting $S = 16$ symbols

Copyright (c) 2014 IEEE. Personal use is permitted. For any other purposes, permission must be obtained from the IEEE by emailing pubs-permissions@ieee.org.

This is the author's version of an article that has been published in this journal. Changes were made to this version by the publisher prior to publication.
The final version of record is available at http://dx.doi.org/10.1109/TSP.2014.2307838

over 1000 Monte Carlo simulations. Due to the reliance on perfectly uncorrelated symbols, the proposed method results in lower sidelobe levels as well as greater attenuation of the interfering target (about 3 dB in this case). Note that the CE waveforms also incur a downward bias of 6.3 dB for the target located at -15° and 4.93 dB for the target located at 15°. In contrast, the proposed architecture results in biases of 1.58 dB and 1.15 dB. Although not pictured, similar results are obtained for $S = 256$ transmitted symbols, as well as with higher noise variance.

VII. Conclusion

We have demonstrated a closed-form method of covariance matrix design for the MIMO transmit beamforming problem that exploits the properties of DFT coefficients. The resulting covariance matrix fulfills both the positive semidefinite and uniform elemental power constraints, is computationally efficient, and results in similar performance to that achieved by iterative solutions. We have also demonstrated a radar architecture that can be used with a set of orthogonal signals to match the desired beampattern. The resulting beampattern matches the theoretical pattern exactly, resulting in superior MSE performance compared to existing methods. The architecture itself is computationally efficient and allows the user to forego the usual preliminary step of designing the covariance matrix.

Appendix A
Orthogonality of $\mathbf{h}_k$'s

Consider $\mathbf{h}_k$ as defined by (14). This yields the resulting inner product

$$\begin{aligned}\mathbf{h}_k^H\mathbf{h}_l &= \frac{H(k)H(l)}{N_T^2}\sum_{n=0}^{N_T-1} e^{j2\pi(l-k)n/N_T} \\ &= \frac{H(k)H(l)}{N_T^2}\frac{1-e^{j2\pi(l-k)}}{1-e^{j2\pi(l-k)/N_T}} \\ &= \frac{H(k)H(l)}{N_T^2}\frac{\sin\left(\pi(l-k)\right)}{\sin\left(\frac{\pi}{N_T}(l-k)\right)}. \end{aligned} \tag{45}$$

The above result is clearly zero for $l \neq k$. In the case of $l = k$, we invoke L'Hopital's rule to find the limit

$$\begin{aligned}&\lim_{(l-k)\to 0}\frac{H(k)H(l)}{N_T^2}\frac{\sin\left(\pi(l-k)\right)}{\sin\left(\frac{\pi}{N_T}(l-k)\right)} \\ &\quad= \lim_{(l-k)\to 0}\frac{H(k)H(l)}{N_T^2}\frac{\pi\cos\left(\pi(l-k)\right)}{\frac{\pi}{N_T}\cos\left(\frac{\pi}{N_T}(l-k)\right)} \\ &\quad= \frac{H(k)^2}{N_T}.\end{aligned}$$

Copyright (c) 2014 IEEE. Personal use is permitted. For any other purposes, permission must be obtained from the IEEE by emailing pubs-permissions@ieee.org.

This is the author's version of an article that has been published in this journal. Changes were made to this version by the publisher prior to publication.
The final version of record is available at http://dx.doi.org/10.1109/TSP.2014.2307838

The final result is then

$$\mathbf{h}_k^H \mathbf{h}_l = \frac{1}{N_T} H(k)^2 \delta_{kl}, \tag{46}$$

where δ_{kl} denotes the Kronecker delta.

APPENDIX B
PROOF OF LEMMA 2

Consider the k-space steering vector defined in (20). Using the fact that $h(n) = h^*(N_T - n)$, it follows that the vector $\mathbf{e}^H(k)\mathbf{R}$ has elements

$$\left[\mathbf{e}^H(k)\mathbf{R}\right]_i = \sum_{n=0}^{N_T-1} h^*(n) e^{j\frac{2\pi k(n+i)}{N_T}}, \; i = 0, ..., N_T - 1. \tag{47}$$

Thus, the power in k-space is

$$\begin{aligned} \mathbf{e}^H(k)\mathbf{R}\mathbf{e}(k) &= N_T \left(\sum_{n=0}^{N_T-1} h(n) e^{-j\frac{2\pi kn}{N_T}} \right)^* \\ &= N_T H^*(k) \\ &= N_T H(k) \end{aligned} \tag{48}$$

APPENDIX C
BW_{NN} FOR PHASED-ARRAY BEAM

For the phased-array beam, the covariance matrix $\mathbf{R} = \mathbf{1}\mathbf{1}^H$, where $\mathbf{1}$ represents the column vector of all ones. The resulting power is

$$\begin{aligned} P(\theta) &= \mathbf{a}_T^H(\theta)\mathbf{1}\mathbf{1}^H\mathbf{a}_T(\theta) \\ &= \sum_{n=0}^{N_T-1} e^{j\frac{2\pi d}{\lambda} n \sin(\theta)} \sum_{m=0}^{N_T-1} e^{-j\frac{2\pi d}{\lambda} m \sin(\theta)} \\ &= \left| \frac{1 - e^{j\frac{2\pi d}{\lambda} N_T \sin(\theta)}}{1 - e^{j\frac{2\pi d}{\lambda} \sin(\theta)}} \right|^2 \\ &= \left| \frac{\sin\left[\frac{\pi d}{\lambda} N_T \sin(\theta)\right]}{\sin\left[\frac{\pi d}{\lambda} \sin(\theta)\right]} \right|^2, \end{aligned} \tag{49}$$

which is the familiar beampattern of the uniformly weighted ULA [24]. The nulls occur where the numerator is minimized and the denominator is not equal to zero. This is true when

$$\frac{\pi d}{\lambda} N_T \sin(\theta) = m\pi, \; m = 1, \ldots, \frac{N_T}{2}, \tag{50}$$

resulting in nulls at the locations

$$\theta = \pm \sin^{-1}\left(\frac{\lambda m}{d N_T}\right), \; m = 1, \ldots, \frac{N_T}{2}. \tag{51}$$

Copyright (c) 2014 IEEE. Personal use is permitted. For any other purposes, permission must be obtained from the IEEE by emailing pubs-permissions@ieee.org.

This is the author's version of an article that has been published in this journal. Changes were made to this version by the publisher prior to publication.
The final version of record is available at http://dx.doi.org/10.1109/TSP.2014.2307838

REFERENCES

[1] E. Fishler, A. Haimovich, R. Blum, D. Chizhik, L. Cimini, and R. Valanzuela, "MIMO Radar: An idea whose time has come," in *Proc. IEEE Radar Conf.*, Honolulu, HI, Apr. 2004, pp. 71–78.

[2] J. Li and P. Stoica, "Target detection and parameter estimation for MIMO radar systems," *IEEE Trans. Aerosp. Electron. Syst.*, vol. 44, no. 3, pp. 927–939, Jul. 2008.

[3] J. Li and P. Stoica, Eds., *MIMO Radar Signal Processing*. Hoboken, NJ: John Wiley & Sons, 2009.

[4] A. Hassanien and S. A. Vorobyov, "Phased-MIMO Radar: A tradeoff between phased-array and MIMO Radars," *IEEE Trans. Signal Process.*, vol. 58, no. 6, pp. 3137–3151, Jun. 2010.

[5] A. Haimovich, R. Blum, and L. Cimini, "MIMO Radar with widely separated antennas," *IEEE Signal Process. Mag.*, vol. 25, no. 1, pp. 116–129, Jan. 2008.

[6] J. Li and P. Stoica, "MIMO Radar with colocated antennas," *IEEE Signal Process. Mag.*, vol. 24, no. 5, pp. 106–114, Sep. 2007.

[7] D. R. Fuhrmann, J. P. Browning, and M. Rangaswamy, "Signaling strategies for the hybrid MIMO phased-array Radar," *IEEE J. Sel. Topics Signal Process.*, vol. 4, no. 1, pp. 66–78, Feb. 2010.

[8] P. Stoica, J. Li, and Y. Xie, "On probing signal design for MIMO Radar," *IEEE Trans. Signal Process.*, vol. 55, no. 8, pp. 4151–4161, Aug. 2007.

[9] T. Aittomaki and V. Koivunen, "Signal covariance matrix optimization for transmit beamforming in MIMO Radars," in *Proc. Asilomar Conference on Signals, Systems, and Computers*, Nov. 2007, pp. 182–186.

[10] ——, "Low-Complexity method for transmit beamforming in MIMO Radars," in *Proc. International Conference on Acoustics, Speech, and Signal Processing (ICASSP)*, 2007, pp. 305–308.

[11] S. Ahmed, J. Thompson, Y. Petillot, and B. Mulgrew, "Unconstrained synthesis of covariance matrix for MIMO Radar transmit beampattern," *IEEE Trans. Signal Process.*, vol. 59, no. 8, pp. 3837–3849, Aug. 2011.

[12] D. R. Fuhrmann and G. S. Antonio, "Transmit beamforming for MIMO Radar systems using signal cross-correlation," *IEEE Trans. Aerosp. Electron. Syst.*, vol. 44, no. 1, pp. 171–186, Jan. 2008.

[13] J. Li and P. Stoica, "Waveform synthesis for diversity-based transmit beampattern design," *IEEE Trans. Signal Process.*, vol. 56, no. 6, pp. 3461–3464, Jun. 2008.

[14] S. Ahmed, J. Thompson, Y. Petillot, and B. Mulgrew, "Finite alphabet constant-envelope waveform design for MIMO Radar transmit beampattern," *IEEE Trans. Signal Process.*, vol. 59, no. 11, pp. 5326–5337, Nov. 2011.

[15] S. Jardak, S. Ahmed, and M.-S. Alouini, "Generating correlated QPSK waveforms by exploiting real gaussian random variables," in *IEEE Asilomar Conference on Signal, System, and Computers*, 2012.

[16] M. Joham, W. Utschick, and J. A. Nossek, "Linear transmit processing in MIMO communications systems," *IEEE Trans. Signal Process.*, vol. 53, no. 8, pp. 2700–2712, Aug. 2005.

[17] J. Proakis and M. Salehi, *Digital Communications*, 5th ed. Boston, MA: McGraw-Hill, 2008.

[18] B. Friedlander, "On transmit beamformign for MIMO radar," *IEEE Trans. Aerosp. Electron. Syst.*, vol. 48, no. 4, pp. 3376–3388, Oct. 2012.

[19] A. Hassanien and S. A. Vorobyov, "Transmit energy focusing for DOA estimation in MIMO radar with colocated antennas," *IEEE Trans. Signal Process.*, vol. 59, no. 6, pp. 2669–2682, Jun. 2011.

[20] G. Hua and S. S. Abeysekera, "Colocated mimo radar transmit beamforming using orthogonal waveforms," in *Proc. 2012 IEEE Int. Conf. Acoustics, Speech, and Signal Processing*, Kyoto, Japan, Mar. 2012, p. 2453.

Copyright (c) 2014 IEEE. Personal use is permitted. For any other purposes, permission must be obtained from the IEEE by emailing pubs-permissions@ieee.org.

This is the author's version of an article that has been published in this journal. Changes were made to this version by the publisher prior to publication.
The final version of record is available at http://dx.doi.org/10.1109/TSP.2014.2307838

[21] M. Grand and S. Boyd, "CVX: Matlab software for disciplined convex programming, version 2.0 beta," http://cvxr.com/cvx, Jul. 2013.

[22] M. Grant and S. Boyd, "Graph implementations for nonsmooth convex programs," in *Recent Advances in Learning and Control*, ser. Lecture Notes in Control and Information Sciences, V. Blondel, S. Boyd, and H. Kimura, Eds. Springer-Verlag Limited, 2008, pp. 95–110.

[23] B. V. Veen and K. Buckley, "Beamforming: A versitile approach to spatial filtering," *IEEE ASSP Mag.*, vol. 5, no. 2, pp. 4–24, Apr. 1988.

[24] H. L. V. Trees, *Optimum Array Processing*. New York, NY: John Wiley & Sons, 2002.

John Lipor is a Ph.D. student at the University of Michigan, Ann Arbor and an awardee of the 2013 NSF Graduate Research Fellowship Program. He earned his BSEE in 2009 from the University of Wisconsin, Madison and MSEE from the King Abdullah University of Science and Technology (KAUST), Thuwal, Kingdom of Saudi Arabia. John's current research interests include adaptive sampling and blind calibration, with applications to environmental sensing.

Sajid Ahmed (M'08, SM'12) received the B.S in Electronics Engineering from Sir Syed University of Engiering and Technology Karachi, Pakistan in 1998 and M. Sc in Communication Engineering from University of Manchester, Institute of Science and Technology, UK in 2002. He completed his PhD in Digital Signal Processing at the King's College London and Cardiff University, UK in 2005. He was a researcher at the Queen's University Belfast, Northern Ireland and the University of Edinburgh, UK. Presently, he is with the King Abdullah University of Science and Technology (KAUST), Thuwal, Kingdom of Saudi Arabia. Dr. Ahmed's current research interests include the linear and non-linear optimization techniques, low complexity parameter estimation for communication and radar systems, passive radar, and waveforms design for MIMO radar.

Copyright (c) 2014 IEEE. Personal use is permitted. For any other purposes, permission must be obtained from the IEEE by emailing pubs-permissions@ieee.org.

This is the author's version of an article that has been published in this journal. Changes were made to this version by the publisher prior to publication.
The final version of record is available at http://dx.doi.org/10.1109/TSP.2014.2307838

Mohamed-Slim Alouini was born in Tunis, Tunisia. He received the Ph.D. degree in Electrical Engineering from the California Institute of Technology (Caltech), Pasadena, CA, USA, in 1998. He served as a faculty member in the University of Minnesota, Minneapolis, MN, USA, then in the Texas A&M University at Qatar, Education City, Doha, Qatar before joining King Abdullah University of Science and Technology (KAUST), Thuwal, Makkah Province, Saudi Arabia as a Professor of Electrical Engineering in 2009. His current research interests include the modeling, design, and performance analysis of wireless communication systems.

Copyright (c) 2014 IEEE. Personal use is permitted. For any other purposes, permission must be obtained from the IEEE by emailing pubs-permissions@ieee.org.